

No. 135/2025 ISSN 2657-6988 (online) ISSN 2657-6988 (online)

Submitted: 21.05.2025 Accepted: 25.06.2025 DOI: 10.26408/135.02 Published: 26.09.2025

CURRENTS OF INDUCTION MOTOR UNDER VOLTAGE FLUCTUATIONS

Damian Hallmann^{1*}. Piotr Gnaciński².

- 1,2 Gdynia Maritime University, Morska 81–87, 81–225 Gdynia, Poland, Faculty of Electrical Engineering, Department of Marine Electrical Power Engineering
- ¹ ORCID 0000-0003-4129-8336, email: d.hallmann@we.umg.edu.pl
- ² ORCID 0000-0003-3903-0453, email: p.gnacinski@we.umg.edu.p

Abstract: Voltage fluctuations are a common occurrence in power systems. They can be regarded as a superposition of the fundamental voltage component, subharmonics and interharmonics - components at frequencies below the fundamental one or not being its integer multiple, respectively. This paper focuses on the effect of the moment of inertia of a driven unit on the subharmonics and interharmonics present in the supply current of a cage induction motor under rectangular voltage modulation. The results of a 2D finite element analysis are presented for a cage induction motor with a rated power of 3 kW.

Keywords: interharmonics, cage induction motor, finite element method, power quality, subharmonics, voltage waveform distortions.

1. INTRODUCTION

One distortion in voltage quality is voltage fluctuations [Bollen and Gu 2006; Kuwałek 2021a.b: 2022: Patel and Chowdhury 2021: Gnaciński et al. 2022: 20241 understood as sudden changes in its RMS value. These changes are most often discrete [Kuwałek 2021a], vet fluctuations with a different trend, such as trapezoidal, also exist [Kuwałek 2021a].

Periodic voltage fluctuations are associated with the presence of subharmonics (subsynchronous interharmonics) and interharmonics in the voltage waveform – that is, components with frequencies respectively less than the fundamental component frequency or not being an integer multiple of that frequency. Sine-wave voltage fluctuations can be considered as a case of simultaneous subharmonics and interharmonics with equal values and frequencies that are symmetrical to the fundamental component [Gallo et al. 2005; Bollen and Gu 2006; Gnaciński et al. 2022; 2024], e.g. 10 Hz and 90 Hz (in a 50 Hz system). Depending on the phase shift angle of the subharmonics and interharmonics [Gallo et al. 2005; Bollen and Gu 2006], a voltage amplitude modulation case, a phase modulation case and an

^{*}Corresponding author

intermediate case can be distinguished [Gallo et al. 2005; Bollen and Gu 2006; Gnaciński et al. 2022; 2024]. Note also that voltage fluctuations of any waveform can be analysed as a superposition of sine fluctuations at different frequencies [Ghaseminezhad et al. 2021b; Gnaciński et al. 2024].

Causes of voltage fluctuations, subharmonics and interharmonics include the operation of time-varying power loads [Bollen and Gu 2006; Li et al. 2012; Zhiyuan 2017; Arkkio et al. 2018; Gutierrez-Ballesteros, Rönnberg and Gil-de-Castro 2022], renewable energy sources [Bollen and Gu 2006; Nambiar, Kiprakis and Wallace 2010; Kovaltchouk et al. 2016; Mao et al. 2024; Xu et al. 2025] and power electronic equipment [Tripp, Kim and Whitney 1993; Zhang, Xu and Liu 2005; Kuwałek and Wilczyński 2021].

Voltage fluctuations and their associated subharmonics and interharmonics interfere with the operation of various electrical units, including lights [Gallo et al. 2005; Bollen and Gu 2006; Gil-de-Castro, Rönnberg and Bollen 2017; Abdalaal and Ho 2021; Kuwałek 2021a,b; 2022; Gutierrez-Ballesteros, Rönnberg and Gil-de-Castro 2022], power electronic, devices [Testa and Langella 2005], control systems [Testa and Langella 2005], power and measurement transformers [Testa and Langella 2005; Crotti et al. 2021], and turbine generating sets [Testa and Langella 2005]. The interference or disturbances under consideration have a particularly detrimental effect on rotating machinery, including induction motors. The effects of voltage, subharmonic and interharmonic fluctuations include local saturation of the magnetic circuit [Ghaseminezhad et al. 2017a,b], flow of subharmonic and interharmonic currents through the windings [Tennakoon, Perera and Robinson 2008; Gnaciński et al. 2019a,b; 2021; 2023; Hallmann 2020], motor overheating and increased power losses [Gallo et al. 2005; Testa and Langella 2005; Ghaseminezhad et al. 2017a,b; 2021a; Gnaciński et al. 2019a; Hallmann 2020], speed fluctuations [Tennakoon, Perera and Robinson 2008; Ghaseminezhad et al. 2017; 2021a; Gnaciński et al. 2021; Zhang, Kang and Yuan 2021], torque fluctuations [Ghaseminezhad et al. 2017; 2021b; Gnaciński et al. 2019a; 2021; 2023; Hallmann 2020], as well as vibrations and torsional oscillations [Tripp, Kim and Whitney 1993; Gnaciński et al. 2019b; 2021; 2023; 2024], which can result in drive coupling rupture, for example [Tripp, Kim and Whitney 1993].

Particularly significant vibrations, torque pulsations, speed fluctuations and values of subharmonics and interharmonics of the current flowing through the motor windings occur with the torsional vibration resonance of a rigid body [Gnaciński et al. 2019a,b; 2021; 2023; 2024; Ghaseminezhad 2021b]. A specific type of resonance occurs when the electromagnetic torque pulsation frequency in a motor or the resistive torque of a driven unit corresponds to the natural frequency of the torsional vibrations of the rotating masses [Arkkio et al. 2018; Gnaciński et al. 2019a,b; 2021; 2023; 2024; Ghaseminezhad 2021b]. For low-power machines, the natural frequency of the torsional vibration in a rigid body is in the order of tens of Hz, while that of high-power machines is in the order of single Hz. For this type of vibration, the angular torsion of the individual rotating components (e.g. coupling, shaft, etc.) is

small, while there are speed fluctuations [Arkkio et al. 2018]. Note that the effect of a motor's electromagnetic torque on the rotating masses can be compared to that of a coil spring [Arkkio et al. 2018].

Although voltage subharmonics and interharmonics are considered to be particularly harmful disturbances to voltage quality, their acceptable limit levels are not specified in the applicable standards [EN Standard 50160:2010; IEEE 519:2014] because there is insufficient experimental data. The information section of the *IEEE Standard for Harmonic Control in Electric Power Systems* [IEEE 519:2014] provides the rationale for establishing acceptable limits for subharmonics and interharmonics and proposes two curves defining the maximum permissible value of subharmonics and interharmonics versus their frequency. In practice, one curve generally limits subharmonics and interharmonics to 0.5% and the other to 0.3%.

Voltage quality regulations and standards limit voltage fluctuations indirectly, through a maximum flicker limit [Bollen and Gu 2006; EN Standard 50160:2010]. As found in the reference literature [Gallo et al. 2005; Gnaciński et al. 2024], this approach does not protect induction motors from the negative effects of subharmonics and interharmonics. In conclusion, the modification of the voltage quality standards and introduction of the subharmonic and interharmonic limits to them demands further research that should focus on induction motors supplied with voltage that features these types of harmonics.

Asynchronous motors under voltage fluctuations and in the presence of subharmonics and interharmonics are the subject of many research works [Tripp, Kim and Whitney 1993; Gallo et al. 2005; Testa and Langella 2005; Tennakoon, Perera and Robinson 2008; Ghaseminezhad et al. 2017a,b; 2021a; Gnaciński et al. 2019a,b; 2021; 2023; Hallmann 2020; Zhang, Kang and Yuan 2021]. They generally ignored the effect of the moment of inertia of driven units on the subharmonics and interharmonics of the motor winding current. The effect of the moment of inertia was considered in [Gnaciński et al. 2019a; Hallmann 2020], yet it was limited to an analysis of the motor under single voltage subharmonic conditions. This work presents the effect of the moment of inertia of a driven unit on the subharmonics and interharmonics of the motor current under rectangular voltage modulation conditions. The work complements the authors' previous publications [Gnaciński et al. 2019a,b; 2021; 2022; 2023; 2024].

2. FIELD MODEL

The study was performed by applying a finite element method to a 3 kW squirrel cage induction motor, selected parameters of which are listed in Table 1. Two-dimensional field calculations were run in ANSYS Electronics Desktop 2022R2.4 (formerly: ANSYS Maxwell).

A preliminary motor model was developed using the RMxprt module, with the model parameters identified from design data provided by the motor manufacturer and empirical tests carried out [Hallmann 2020]. On the basis of a convergence analysis [Hallmann 2020], the subdivision grid was significantly denser than that proposed in the RMxprt module. The original subdivision grid featured around 5,000 elements, while the denser one increased the number to 22,000. After the densification, the maximum finite element length was as follows: 2.46 mm for the shaft; 4.95 mm for the stator; 2.46 mm for the rotor; 2.25 mm for the stator windings; 0.79 mm for the aluminium cage; 0.74 mm for the motor gap; 2.49 mm for all other components modelled. The tau subdivision grid used is illustrated in Figure 1.

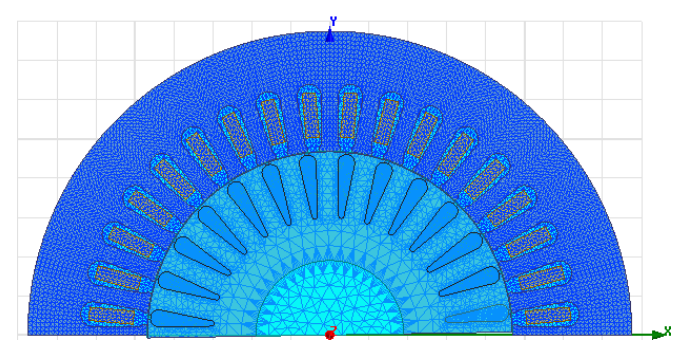


Fig. 1. Mesh used

Source: [Gnaciński and Hallmann 2024].

Table 1. Selected parameters of the test motor type TSg 100L-4B

Specification	Value
Nominal power [kW]	3
Rated voltage [V]	380
Rated current [A]	6.9
Rated power factor [-]	0.81
Rated speed [rpm]	1420
Moment of inertia [kg m²]	0.00702299
Winding connection system	Delta

Numerical calculations were completed using a transient solver. The effects of vibration and deformation were not taken into account in the calculations. The stator and rotor winding temperatures were determined using a thermal equivalent motor diagram [Gnaciński et al. 2019a].

The experimental validation and a more detailed description of the model are in the authors' earlier works, like [Gnaciński et al. 2019a; 2021; Hallmann 2020].

3. RESULTS

The results for an induction motor with rectangular supply voltage modulation are shown below. The numerical experiments were performed for a rated load torque and two different values of motor-to-driven-unit moment of inertia ratios (j): j = 0 (negligible moment of inertia) and j = 5.

An example of the RMS voltage waveform for modulation frequency $f_m = 30$ Hz is given in Figure 2. The voltage change [Gnaciński et al. 2024] was u = 0.94% for this modulation. Figure 3 shows the voltage spectrum for this modulation. It contains subharmonics and interharmonics with frequencies described by the relationships (based on [Gallo et al. 2005; Zhang, Xu and Liu 2005; Bollen and Gu 2006; Gnaciński et al. 2024]):

$$f_{sh} = f_1 - nf_m \tag{1}$$

$$f_{ih} = f_1 + nf_m \tag{2}$$

with: $n = 1, 2, 3..., f_{sh}, f_{ih}$ - the subharmonic and interharmonic frequencies, respectively, corresponding to the *n*-th harmonic frequency of the modulating function, f_m .

If the frequency determined by (1) is negative, the subharmonic should be assumed to be of opposite order [Zhang, Xu and Liu 2005]. Note also that for the assumed voltage variation u = 0.94%, the subharmonic and interharmonic corresponding to the 1st harmonic of the modulating function assume 0.3%.

As mentioned in the Introduction, this is, in simple terms, the maximum permissible value of subharmonics according to one of the proposals in the *IEEE Standard for Harmonic Control in Electric Power Systems* [IEEE Standard 519:2014].

Figure 4 shows the current waveform for j = 0, corresponding to the voltage modulation from Figure 2, and Figure 5 shows the current spectrum. The current contained the following subharmonics and interharmonics: $f_{sh} = 30 \text{ Hz}$, $i_{sh} = 25.24\%$, $f_{ih} = 80 \text{ Hz}$, and $i_{sh} = 12.55\%$. Note that for the motor under test, the subharmonic at frequency $f_{sh} = 20 \text{ Hz}$ corresponded to the resonant frequency of the torsional vibration of a rigid body.

In turn, the total nonharmonic distortion rate [Arranz-Gimon et al. 2021], TnHD, understood as:

$$TnHD = \frac{\sqrt{I_{RMS} - \sum_{h=0}^{h_{max}} (I_h)^2}}{I_1}$$
(3)

was equal to TnHD = 28.1%, with: I_{RMS} – current RMS value, I_1 , I_h – fundamental harmonic of the h-th current harmonic.

An analogous current spectrum for j = 5 and modulation frequency $f_m = 30$ Hz is shown in Figure 6. Here, the current subharmonics and interharmonics were much lower: $f_{sh} = 30$ Hz, $i_{sh} = 9.72\%$, $f_{ih} = 80$ Hz, and $i_{sh} = 1.27\%$, whereas TnHD = 12.5%. This was due to the fact that torsional vibration resonance of the rigid body did not occur for large moments of inertia [Gnaciński et al. 2019a].

The following charts show the current spectra for $f_m = 9$ Hz, j = 0 (Fig. 7), $f_m = 9$ Hz, j = 5 (Fig. 8), $f_m = 20$ Hz, j = 0 (Fig. 9), $f_m = 20$ Hz, j = 5 (Fig. 10), and $f_m = 40$ Hz, j = 0 (Fig. 11) and j = 5 (Fig. 12). The TnHD values for the current waveforms are listed in Table 2.

For a negligible moment of inertia of the driven unit (j = 0), TnHD took on the largest value at the modulation frequency $f_m = 30$ Hz (TnHD = 28.1%) and the lowest value at $f_m = 3$ Hz (TnHD = 8.5%). In contrast, when j = 5, TnHD took on the largest value at the modulation frequency $f_m = 30$ Hz (TnHD = 12.5%) and the lowest value at $f_m = 3$ Hz (TnHD = 8.1%). Note that TnHD took on higher values at j = 0 than at j = 5, with the exception of the modulation frequency $f_m = 20$ Hz. For this modulation frequency, TnHD was 10.3% and 11.1%, for j = 0 and j = 5, respectively. The higher value of TnHD for j = 5 was due to the higher value of the subharmonic at $f_{sh} = 30$ Hz for j = 5 ($i_{sh} = 7.72\%$ – Fig. 10) than for j = 0 ($i_{sh} = 5.45\%$ – Fig. 9).

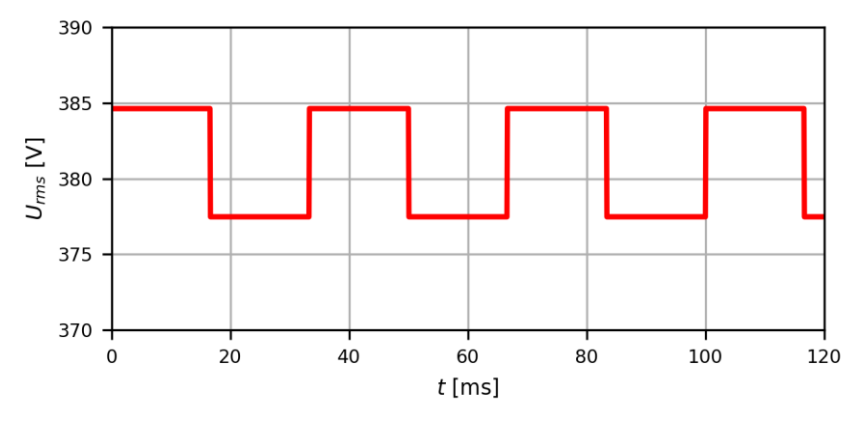


Fig. 2. Supply voltage RMS value for the modulation frequency $f_m = 30 \text{ Hz}$

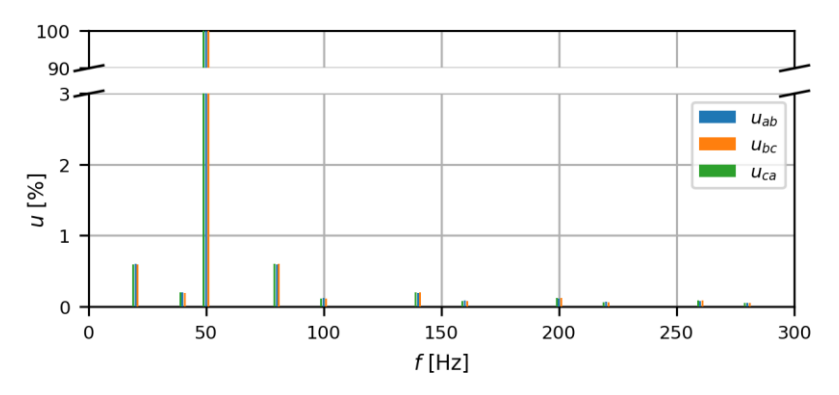


Fig. 3. Supply voltage spectrum for the modulation frequency $f_m = 30 \text{ Hz}$

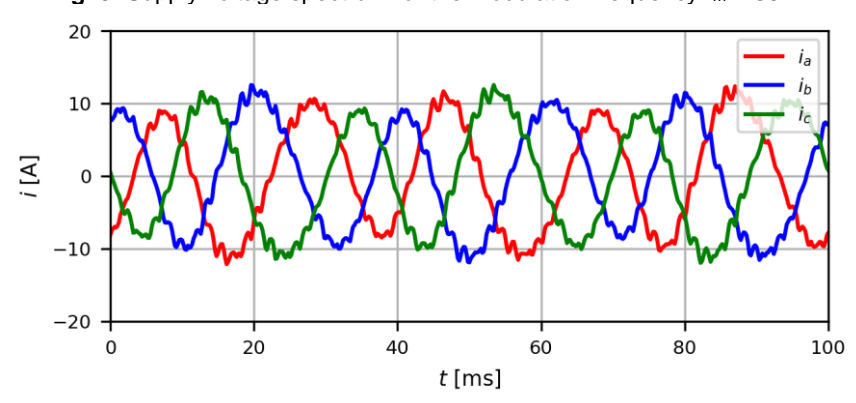


Fig. 4. Example of motor current waveform for the modulation frequency $f_m = 30$ Hz and negligible moment of inertia of the driven unit (j = 0)

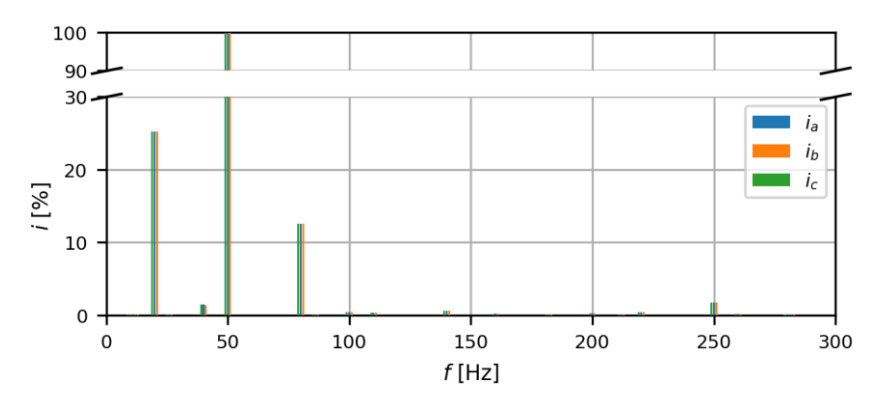


Fig. 5. Spectrum for the current in Figure 4

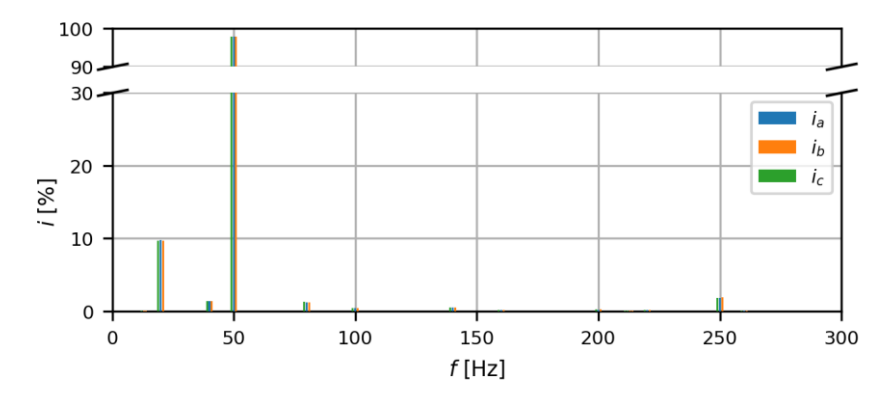


Fig. 6. Spectrum of the motor current draw for the modulation frequency $f_m = 30$ Hz and relative moment of inertia of the driven unit (related to the motor's moment of inertia), j = 5

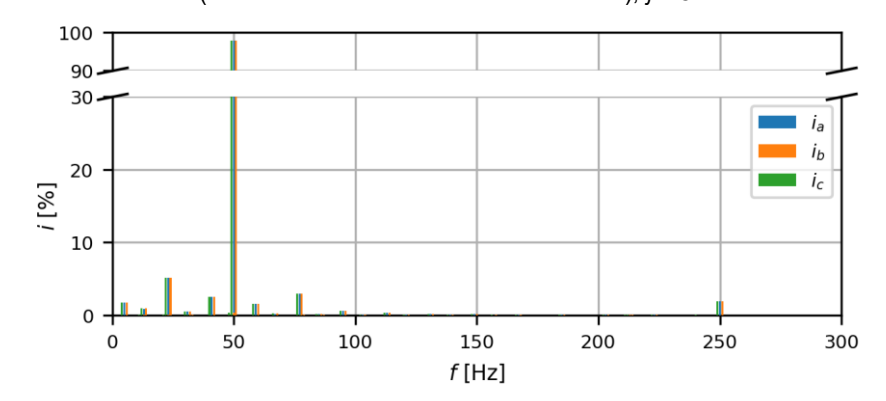


Fig. 7. Spectrum of the motor current draw for the modulation frequency $f_m = 9$ Hz and a negligible moment of inertia of the driven unit, j = 0

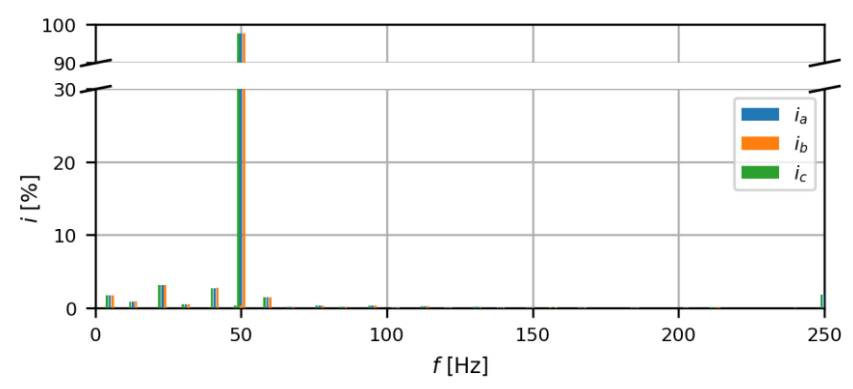


Fig. 8. Spectrum of the motor current draw for the modulation frequency $f_m = 9$ Hz and relative moment of inertia of the driven unit (related to the motor's moment of inertia), j = 5

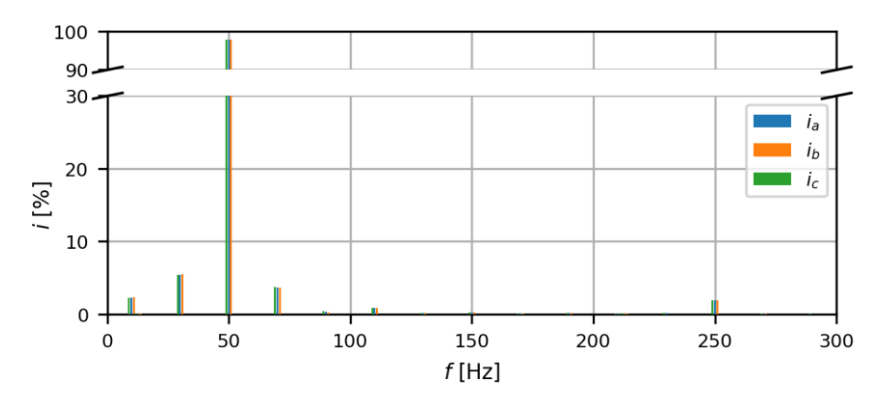


Fig. 9. Spectrum of the motor current draw for the modulation frequency $f_m = 20 \text{ Hz}$ and a negligible moment of inertia of the driven unit, j = 0

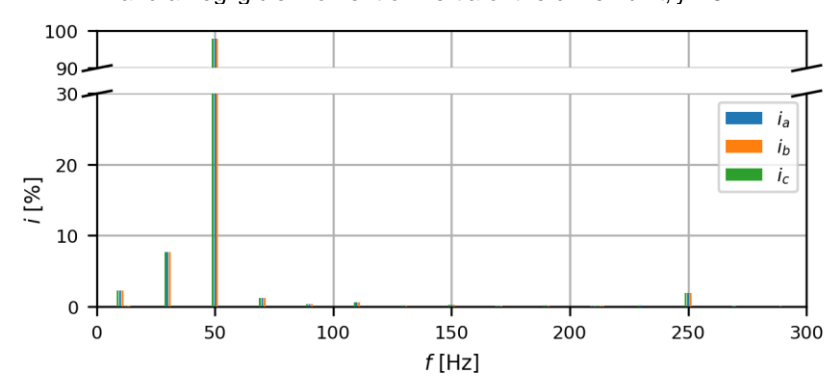


Fig. 10. Spectrum of the motor current draw for the modulation frequency $f_m = 20$ Hz and relative moment of inertia of the driven unit (related to the motor's moment of inertia), j = 5

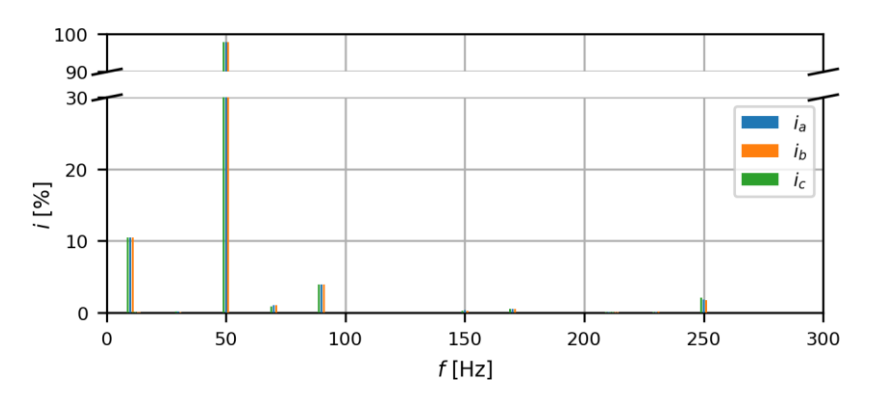


Fig. 11. Spectrum of the motor current draw for the modulation frequency $f_m = 40$ Hz and a negligible moment of inertia of the driven unit, j = 0

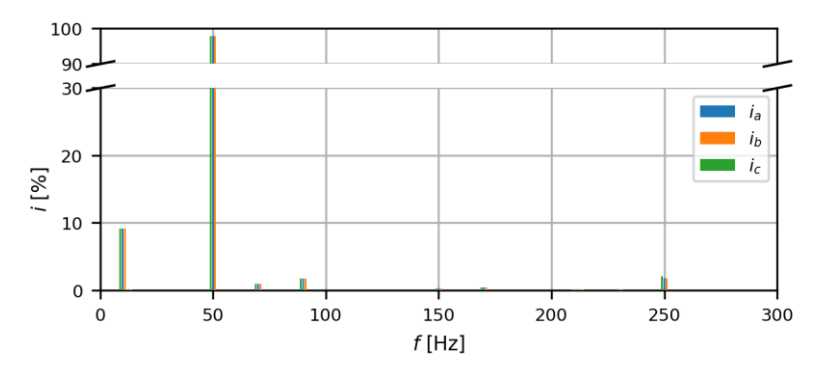


Fig. 12. Spectrum of the motor current draw for the modulation frequency $f_m = 40$ Hz and relative moment of inertia of the driven unit (related to the motor's moment of inertia). i = 5

Table 2. TnHD of the motor current for different modulation frequencies and relative moments of inertia of the driven unit, *j* (related to the motor's moment of inertia)

Modulation frequency [Hz]	TnHD [%]	
	<i>j</i> = 0	<i>j</i> = 5
3	8.47	8.14
9	10.35	8.98
20	10.35	11.14
30	28.1	12.51
40	13.61	12.11

It should be added that for a voltage subharmonic frequency higher than the resonant frequency, the current subharmonic can assume higher values at large moments of inertia of the driven unit than for a negligible moment of inertia [Gnaciński et al. 2019a].

In summary, the moment of inertia of the driven unit has a significant impact on the value of TnHD. Its value significantly depends on the modulation frequency.

4. CONCLUSIONS

This work presents the results of a study on the effect of the moment of inertia of a motor's driven unit on the subharmonics and interharmonics of the current of a squirrel-cage induction motor under rectangular voltage modulation. The results demonstrate that the moment of inertia had a significant effect on the motor current TnHD. For a negligible moment of inertia, TnHD could be more than twice as high as for the moment of inertia five times that of the motor. A higher TnHD in practice

means that the motor is more susceptible to overheating, torque pulsations and vibrations.

REFERENCES

- Abdalaal, R.M., Ho, C.N.M., 2021, Characterization of Commercial LED Lamps for Power Quality Studies, IEEE Canadian Journal of Electrical and Computer Engineering, vol. 44, no. 2, pp. 94–104.
- Arkkio, A., Cederström, S., Awan, H.A.A., Saarakkala, S.E., Holopainen, T.P., 2018, Additional Losses of Electrical Machines under Torsional Vibration, IEEE Transactions on Energy Conversion, vol. 33, no. 1, pp. 245–251.
- Arranz-Gimon, A., Zorita-Lamadrid, A., Morinigo-Sotelo, D., Duque-Perez, O., 2021, A Review of Total Harmonic Ddistortion Factors for the Measurement of Harmonic and Interharmonic Pollution in Modern Power Systems, Energies, vol. 14, no. 20, pp. 1–38.
- Bollen, M.H.J., Gu, I.Y.H., 2006, Signal Processing of Power Quality Disturbances, Wiley, New York, USA.
- Crotti, G., D'Avanzo, G., Letizia, P.S., Luiso, M., 2021, Measuring Harmonics with Inductive Voltage Transformers in Presence of Ssubharmonics, IEEE Transactions on Instrumentation and Measurement, vol. 70, pp. 1–13.
- EN Standard 50160: 2010, Voltage Characteristics of Electricity Supplied by Public Distribution Network.
- Gallo, D., Landi, C., Langella, R., Testa, A., 2005, *Limits for Low Frequency Interharmonic Voltages: Can They Be Based on the Flickermeter Use*, IEEE Russia Power Tech, pp. 1–7.
- Ghaseminezhad, M., Doroudi, A., Hosseinian, S.H., Jalilian, A., 2017b, Analysis of Voltage Fluctuation Impact on Induction Motors by an Innovative Equivalent Circuit Considering the Speed Changes, IET Generation Transmission Distribution vol. 11, pp. 512–519.
- Ghaseminezhad, M., Doroudi, A., Hosseinian, S.H., Jalilian, A., 2017b, An Investigation of Induction Motor Saturation under Voltage Fluctuation Conditions, Journal of Magnetics, vol. 22, pp. 306–314.
- Ghaseminezhad, M., Doroudi, A., Hosseinian, S.H., Jalilian, A., 2021a, Analytical Feld Study on Induction Motors under Fluctuated Voltages, Iranian Journal of Electrical and Electronic Engineering, vol. 17, no 1, pp. 1620–1620.
- Ghaseminezhad, M., Doroudi, A., Hosseinian, S.H., Jalilian, A., 2021b, *High Torque and Excessive Vibration on the Induction Motors under Special Voltage Fluctuation Conditions*, COMPEL The International Journal for Computation and Mathematics in Electrical and Electronic Engineering, vol. 40, no. 4, pp. 822–836.
- Gil-de-Castro, A., Rönnberg, S.K., Bollen, M.H., 2017, Light Iintensity Variation (Flicker) and Harmonic Emission Related to LED Lamps, Electric Power Systems Research, vol. 146, pp. 107–114.
- Gnaciński, P., Hallmann, D., 2024, *Effect of Mains Communication Voltage on Induction Motors*, Scientific Journal of Gdynia Maritime University, no. 132, pp. 20–34.
- Gnaciński, P., Hallmann, D., Klimczak, P., Muc, A., Pepliński, M., 2021, Effects of Voltage Interharmonics on Cage Induction Motors, Energies, no. 14, no. 5.
- Gnaciński, P., Hallmann, D., Muc, A., Klimczak, P., Pepliński, M., 2022, Induction Motor Supplied with Voltage Containing Symmetrical Subharmonics and Interharmonics, Energies, vol. 15, no. 20, pp. 1–24.
- Gnaciński, P., Hallmann, D., Pepliński, M., Jankowski, P., 2019a, The Effects of Voltage Subharmonics on Cage Induction Machine, International Journal of Electrical Power & Energy Systems, vol. 111, pp. 125–131.
- Gnaciński, P., Pepliński, M., Muc, A., Hallmann, D., Jankowski, P., 2023, Effect of Ripple Control on Induction Motors, Energies, vol. 16, no. 23, pp. 1–12.
- Gnaciński, P., Pepliński, M., Muc, A., Hallmann, D., Klimczak, P., 2024, Induction Motors under Voltage Fluctuations and Power Quality Standards, IEEE Transactions on Energy Conversion, vol. 39, no. 2, pp. 1255–1264.
- Gnaciński, P., Pepliński, M., Murawski, L., Szeleziński, A., 2019b, Vibration of Induction Machine Supplied with Voltage Containing Subharmonics and Interharmonics, IEEE Transactions Energy Con-vers., vol. 34, pp. 1928– 1937.

- Gutierrez-Ballesteros, E., Rönnberg, S., Gil-de-Castro, A., 2022, Characteristics of Voltage Fluctuations Induced by Household Devices and the Impact on LED Lamps, International Journal of Electrical Power & Energy Systems, vol. 141, pp. 1–13.
- IEEE Standard 519:2014 (Revision of IEEE Standard 519:1992), 2014, IEEE Recommended Practice and Requirements for Harmonic Control in Electric Power Systems, New York, USA.
- Kovaltchouk, T., Armstrong, S., Blavette, A., Ahmed, H.B., Multon, B., 2016, Waveform Flicker Severity: Comparative Analysis and Solutions, Renewable Energy, vol. 91, pp. 32–39.
- Kuwałek, P., 2021a, Estimation of Parameters Associated with Individual Sources of Voltage Fluctuations, IEEE Transactions on Power Delivery, vol. 36, no. 1, pp. 351–361.
- Kuwałek, P., 2021b, Selective Identification and Localization of Voltage Fluctuation Sources in Power Grids, Energies, vol. 14, no. 20.
- Kuwałek, P., 2022, IEC Flickermeter Measurement Results for Distorted Modulating Signal while Supplied with Distorted Voltage, 20th International Conference on Harmonics & Quality of Power (ICHQP), pp. 1–6.
- Kuwałek, P., Wilczyński, G., 2021, Dependence of Voltage Fluctuation Severity on Clipped Sinewave Distortion of Voltage, IEEE Transactions Instrumentation and Measure, vol. 70, pp. 1–8.
- Mao, M., Xu, Z., Yuan, Q., Li, H., 2024, Current Interharmonic Prediction Control Based on MPC and Lyapunov for Grid-Connected PV System, IEEE Journal of Emerging and Selected Topics in Power Electronics, vol. 12, no. 3, pp. 2686–2696.
- Nambiar, A.J., Kiprakis, A.E., Wallace, A.R., 2010, Quantification of Voltage Fluctuations Caused by a Wave Farm Connected to Weak, Rural Electricity Networks, Proceedings of 14th International Conference on Harmonics and Quality of Power-ICHQP, pp. 1–8.
- Patel, D., Chowdhury, A., 2021, Mitigation of Voltage Fluctuation in Distribution System using Sen Transformer with Variable Loading Conditions, International Conference on Advances in Electrical, Computing, Communication and Sustainable Technologies (ICAECT), pp. 1–6.
- Tennakoon, S., Perera, S., Robinson, D., 2008, Flicker Attenuation, Part I: Response of Three-Phase Induction Motors to Regular Voltage Fluctuations, IEEE Transactions Power Delivery, vol. 23, pp. 1207–1214.
- Testa, A., Langella, R., 2005, *Power System Subharmonics*, IEEE Power Engineering Society General Meeting, pp. 2237–2242.
- Tripp, H., Kim, D., Whitney, R., 1993, A Comprehensive Cause Analysis of a Coupling Failure Induced by Torsional Oscillations in a Variable Speed Motor, Proceedings of the 22nd Turbomachinery Symposium, Texas A&M University, Turbomachinery Laboratories, pp.17–24.
- Xu, W., Yong, J., Marquez, H.J., Li, C., 2025, *Interharmonic Power A New Concept for Power System Oscillation Source Location*, IEEE Transactions on Power Systems, pp. 1–13.
- Zhang, D., Xu, W., Liu, Y., 2005, On the Phase Sequence Characteristics of Interharmonics, IEEE Transactions on Power Delivery, vol. 20, no. 4, pp. 2563–2569.
- Zhang, S., Kang, J., Yuan, J., 2021, *Analysis and Suppression of Oscillation in V/F Controlled Induction Motor Drive Systems*, IEEE Transactions on Transportation Electrification, vol. 8, pp. 1566–1574.
- Zhiyuan, M., Xiong, M.W., Le, L., Zhong, X., 2017, *Interharmonics Analysis of a 7.5 kW Air Compressor Motor*, International Conference & Exhibition on Electricity Distribution (CIRED), vol. 2017, no. 1, pp. 738–741.

The article is available in open access and licensed under a Creative Commons Attribution 4.0 International (CC BY 4.0)